Mechanism of Pyridine Protonation in Water Clusters of Increasing Size

M. Carmen Sicilia, Alfonso Niño, and Camelia Muñoz-Caro*

Grupo de Química Computacional y Computación de Alto Rendimiento (QCyCAR), E. S. Informática, Universidad de Castilla-La Mancha, Paseo de la Universidad, 4. 13071 Ciudad Real, Spain

Received: January 31, 2005; In Final Form: July 10, 2005

This work presents a theoretical mechanistic study of the protonation of pyridine in water clusters, at the B3LYP/cc-pVDZ theory level. Clusters from one to five water molecules were used. Starting from previously determined structures, the reaction paths for the protonation process were identified. For complexes of pyridine with water clusters of up to three water molecules just one transition state (TS) links the solvated and protonated forms. It is found that the activation energy decreases with the number of water molecules. For complexes of four and five water molecules two transition states are found. For four water molecules, the first TS links the starting solvated structure with a new, less stable, solvated form through a concerted proton transfer between a ring of water molecules. The second TS links the new solvated structure to the protonated form. Thus, protonation is a two-step process. For the five water molecules cluster, the new solvated structure is more stable than the starting one. This structure exhibits two double hydrogen bonds involving the pyridinic nitrogen and several water molecules. The second TS links the new structure with the protonated form. Now the process occurs in one step. In all cases considered, the proton transfers involve an interconversion between covalent and hydrogen bonds. For four and five water molecules, the second TS is structurally and energetically very close to the protonated form. As evidenced by the vibration frequencies, this is due to a flat potential energy hypersurface in the direction of the reaction coordinate. Determination of ΔG at 298.15 K and 1 atm shows that the protonation of pyridine needs at least four water molecules to be spontaneous. The complex with five water molecules exhibits a large ΔG. This value yields a pK_a of 2.35, relatively close to the reported 5.21 for pyridine in water.

Introduction

The mechanism of proton transfer in aqueous solution is an important issue for modeling the physicochemical activity of basic or acidic compounds in a wide range of chemical and biological problems. The most clear example is the ability of a basic or acidic drug to cross cellular membranes, because only neutral species can traverse the lipidic cell structure. Thus, for instance, the protonation capability, described by the pK_a, is one factor determining the biological activity of aminopyridines in the K^+ channel blocking in neural cells.[1]

When considering the effect of the solvent in a given process, such as a protonation, we can perform a partition of the problem.[2] First, we can consider short range effects, which are associated to the direct interaction of solvent molecules with the solute. Second, we have large range effects, electrostatic in nature, which appear as a consequence of the existence of a bulk solvent. Clearly, the mechanistic interpretation of the protonation of an organic base in aqueous solution needs to simulate specifically the short-range effects. Continuum models of solvent consider on equal footing both effects, not allowing for specific interactions between solvent molecules and the solute. It is possible to merge both standpoints by using a hybrid supermolecular-polarizable continuum approach. This approach has been applied to the study of reaction pathways and energy barriers for the alkaline hydrolysis of methyl acetate and formate in water, considering clusters of four water molecules.[3] The energetic results are consistent with the experimental data, particularly the value of the energy barriers for the first step of the hydrolysis in aqueous solution. The previous reasons suggest that the short range effects associated to the proton transfer can be properly described using supermolecular models involving water clusters. Thus, some light on the mechanics of protonation in aqueous solution can be shed by considering complexes with water clusters of increasing size. In addition, this kind of study could evidence the differences arising when going from protonation in a vacuum to solution. Several experimental and theoretical works have been carried out on the stabilization of ionic species in clusters of water molecules. Thus, the HF, MP2 and BLYP levels of theory have been used to analyze dissociation of water molecules, founding that it is achieved in clusters of five and eight water molecules.[4] Also, the HF, DFT and MP2 theory levels have been applied to the study of the ionic dissociation of HF, HCl and H_2S in water clusters.[5] This study shows that four water molecules stabilize the dissociated species. Milet at al.,[6] working at the B3LYP/aug-cc-pVDZ level, have considered the structures of dissociated HCl in clusters of four and five water molecules. On the other hand, molecular dynamics simulations show that the solvation of Na^+ in water needs an average of 5.2 water molecules.[7] Calculations at the DFT level for HBr in clusters of up to four water molecules[8] indicate that HBr does not dissociate until at least three, better four, water molecules are available. Using multicomponent and standard molecular orbital methods, with the 6-31G(d,p) basis set, Tachikawa[9] has studied protonated and deuterated hydrogen fluoride and bromide, in water clusters of up to four water molecules. This work shows that hydrogen fluoride and bromide

* Corresponding author. E-mail: camelia.munoz@uclm.es.

10.1021/jp050530n CCC: $30.25
Published on Web 08/27/2005

can dissociate in clusters of four water molecules. On the experimental side, Amirand and Maillard performed argon-matrix studies on HCl, showing that the molecule is in ionic form for clusters of at least four water molecules.[10] Hurley et al.[11] have used femtosecond pump−probe spectroscopy to show that five water molecules are needed for a complete dissolution of hydrogen bromide to form the contact ion-pair $H^+ \cdot Br^-(H_2O)_5$. Photoelectron spectroscopy has been applied to the sulfate anion, SO_4^{2-}, finding that its double charge is stabilized in the gas phase when accompanied by at least of four water molecules.[12] All these studies suggest that a minimum of four or five water molecules are needed to stabilize ionic species. In this context, we have recently considered the problem of the protonation of pyridine in water clusters of one to five molecules,[13] by working at the B3LYP/cc-pVDZ theory level. Pyridine was used as a representative case due to its intrinsic interest as a prototypical organic base, to its lack of conformational degrees of freedom, and to its relationship with the K^+ channel blockers aminopyridines, whose action depends on the protonation equilibria.[14] The results show that pyridine complexes with clusters of four and five water molecules differ significantly, from the structural and electronic standpoint, from complexes with a smaller number of water molecules.

Related to the previous studies, the hydration of protonated substituted pyridines, up to three water molecules, has been experimentally studied by high-pressure mass spectrometry (HPMS).[15] These works, and previous ones,[16] found a linear relationship between the proton affinity and the basicity in aqueous solution for substituted pyridines, when steric hindrance is unimportant.

In this work, we present a theoretical mechanistic study of the protonation process of pyridine in water clusters of up to five water molecules. Thus, transition states and reaction paths are determined for the protonation process in the five supermolecular models. The problem is considered in energetic and thermodynamical terms. In addition, the variation of pK_a with the size of the water clusters is analyzed.

Theoretical Details

The unprotonated (solvated) and protonated pyridine in water clusters, are described by supermolecular models. Exploration of the potential energy hypersurface, and determination of the reaction path from the solvated to the protonated forms, are carried out in two steps. First, the CHAIN method[17] is applied at the semi ab initio (SAM1) semiempirical electronic structure level,[18] starting from the unprotonated and protonated structures previously obtained;[13] see Figure 1. The CHAIN method works by stepping along the total energy gradient vector field of an arbitrary continuous path between reactants and products.[17] On the other hand, SAM1 is selected because it describes two-electron repulsion integrals more accurately than other semiempirical methods, such as AM1 or PM3. It has been found that SAM1 is able to describe properly hydrogen bonded complexes.[19] In particular, in a previous work,[13] SAM1 has proven its validity to generate initial structures for supermolecular models involving unprotonated and protonated pyridine in clusters of water molecules. The found transition state structures, as well as any new intermediate minima, are refined, considering all the structural degrees of freedom, at the SAM1 level. All these calculations are carried out with the AMPAC package.[20]

In the second step of the analysis, the supermolecular structures determined from the CHAIN method (minima and first order saddle points) are considered at the B3LYP/cc-pVDZ level. These structures are fully relaxed to the closer stationary point. The nature of the saddle points has been determined by computing vibrational frequencies and determining the existence of only one negative value. Starting from the saddle points, the reaction coordinate has been followed forward and backward to determine the proper identity of the corresponding minima. All the calculations have been performed with the Gaussian 03 package.[21] To characterize the molecular structures, the atoms in molecules (AIM) theory[22] is applied from the corresponding one-electron density, ρ. The AIM theory is applied with the Morphy 98 package.[23] Finally, molecular similarity studies are performed using the Carbó-like index defined in the Hex package.[24,25]

The AMPAC and Hex packages have been applied on a standard PC running Windows XP. Gaussian has been applied on a grid of two clusters of twelve PC's each (Pentium IV, 2.4−3.0 GHz, 1 MB RAM), running the clustering administration and configuration system Rocks.[26] Morphy was applied on a Compaq Alphastation running True64 UNIX.

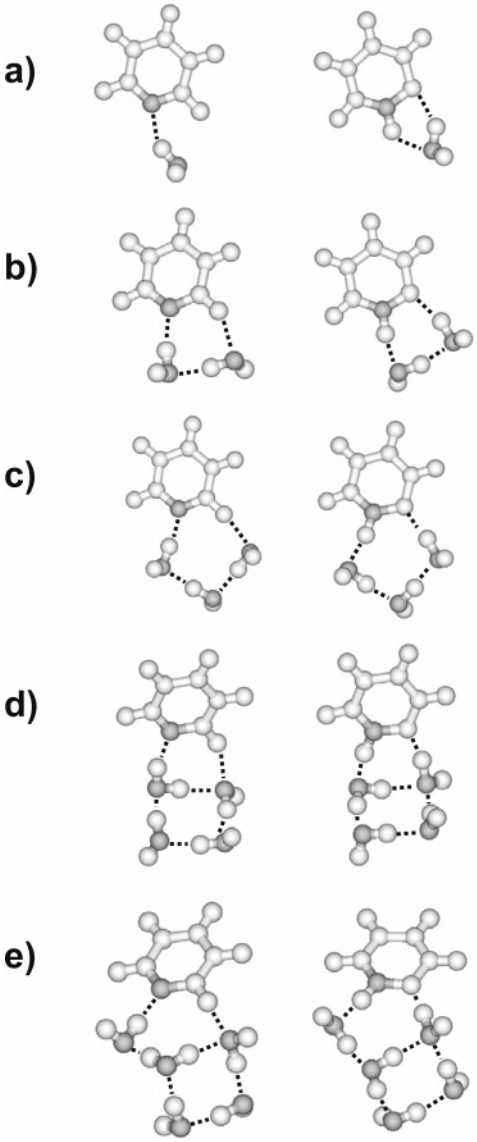

Figure 1. Starting structures for the pyridine−water complexes considered in this work, determined at the B3LYP/cc-pVDZ level in ref 13. Complexes (a)−(e) correspond to water clusters of 1−5 water molecules, respectively. To the left are the purely solvated (unprotonated) structures. To the right are the protonated structures. Dashed lines correspond to bonding interactions identified by the AIM analysis.

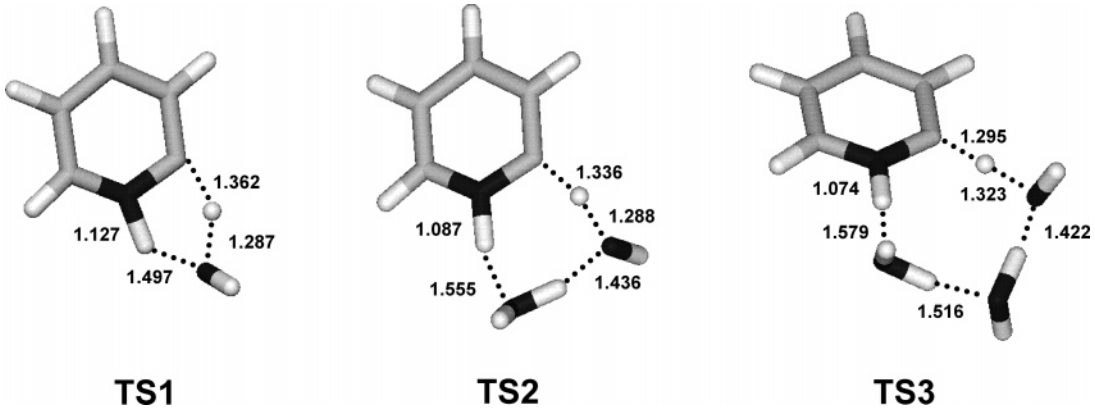

Figure 2. Value of the most relevant distances in the transition state (TS) for the protonation of pyridine in clusters of water molecules, Pyr·nH$_2$O with $n = 1-3$. Data were obtained at the B3LYP/cc-pVDZ level. Dashed lines correspond to bonding interactions as indicated by the AIM analysis (see text). All distances are in angstroms.

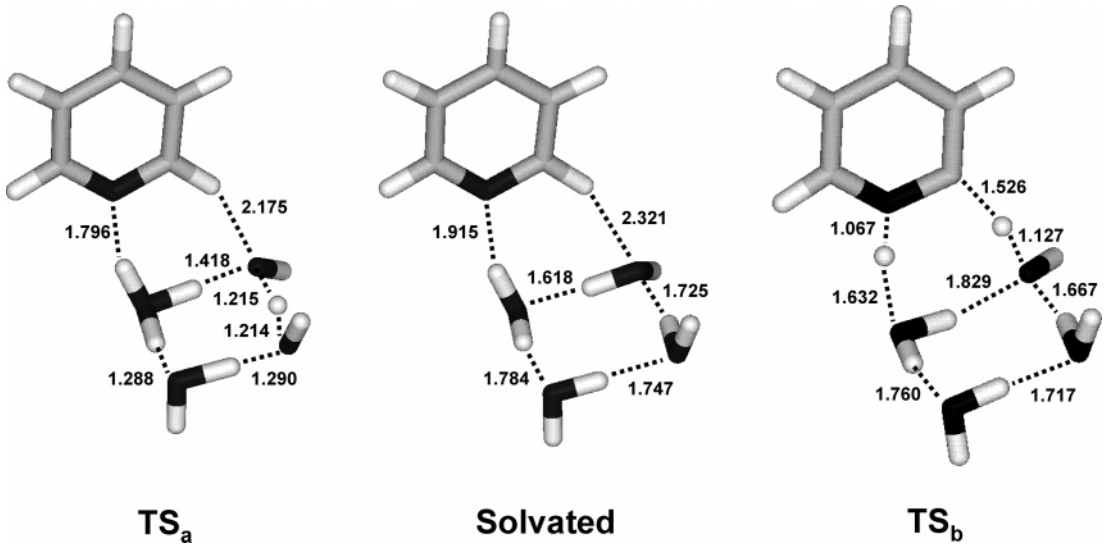

Figure 3. Value of the most relevant distances in the two transition states (TS$_a$, TS$_b$) and the new solvated structure found for the protonation of pyridine in clusters of four water molecules, Pyr·4H$_2$O. Data were obtained at the B3LYP/cc-pVDZ level. Dashed lines correspond to bonding interactions as indicated by the AIM analysis (see text). All distances are in angstroms.

Results and Discussion

The protonation of pyridine (Pyr) in clusters of "n" water molecules is described by the reaction

$$\text{Pyr} + n\text{H}_2\text{O} \rightleftarrows \text{Pyr-H}^+ \cdot \text{OH}^- \cdot (n\text{-}1)\text{H}_2\text{O} \qquad (1)$$

Equation 1 describes a hydrated or solvated pyridine molecule, which protonates by abstracting one proton from a water molecule.

To determine the path on the potential energy hypersurface linking reactants (unprotonated structures) and products (protonated pyridine forms) the CHAIN method[17] is used at the semi ab initio SAM1 level.[18] Five supermolecular models for pyridine, in water clusters up to five water molecules, are considered. The starting solvated (unprotonated) and protonated structures are those previously found by simulated annealing;[13] see Figure 1. Discussion of these ten structures is extensively done in ref 13 and will not be considered here. The SAM1 transition states determined by the CHAIN method[17] are refined at the B3LYP/cc-pVDZ theory level.

For clusters up to three water molecules, just one transition state is found between the unprotonated and protonated systems; see Figure 2. However, two transition states (TS$_a$, TS$_b$) appear in clusters of four and five water molecules, with a new minimum between them, corresponding to a solvated, unprotonated form; see Figures 3 and 4. In all the structures found, as well as in the solvated and protonated forms described in ref 13, the cluster of water molecules binds to pyridine by two anchor points. These are the pyridinic nitrogen and the hydrogen placed in ortho in the pyridinic ring. Fernandez-Berridi et al.,[27] by working at the B3LYP/6-311++G(d,p) theory level, have found that these same anchor points are used to form the most stable complex between pyridine and formic acid.

To analyze the new molecular structures, the atoms in molecules theory (AIM) is applied. The AIM characterizes a bond by an atomic interaction line (AIL), that is a line through the electron density, ρ, along which ρ is a maximum with respect to any neighboring line.[22] On the AIL we find the bond critical point (BCP). This is a second-order saddle point where ρ reaches a minimum.[22] The value of the electronic density at the BCP for a given bond, ρ_b, can be correlated to the concept of bond order,[22] with higher values of ρ_b corresponding to higher degrees of conjugation. In addition, the sign of the Laplacian at the BCP, $\nabla^2\rho_b$, defines the kind of interaction. A negative value arises from an electronic charge concentrated in the internuclear region and therefore shared by the two nuclei. This case defines a shared interaction, typical of a covalent bond,[22] with ρ_b values in the range of 10^{-1} atomic units. On the other hand, a positive

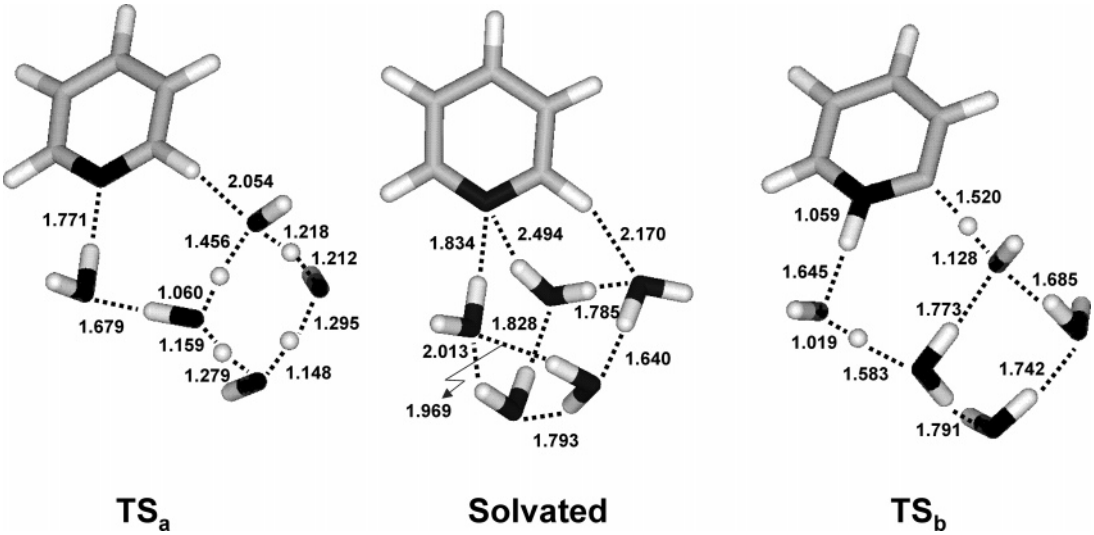

Figure 4. Value of the most relevant distances in the two transition states (TS_a, TS_b) and the new solvated structure found for the protonation of pyridine in clusters of five water molecules, Pyr·5H_2O. Data were obtained at the B3LYP/cc-pVDZ level. Dashed lines correspond to bonding interactions as indicated by the AIM analysis (see text). All distances are in angstroms.

$\nabla^2\rho_b$ evidences an electronic charge contracted toward the nuclei. This is a closed-shell, noncovalent, essentially electrostatic interaction typical of ionic, hydrogen bond, and van der Waals interactions. In this case, ρ_b values are in the range of 10^{-2} atomic units. In addition, AIM identifies rings in molecules through the so-called ring critical point (RCP). An RCP is a critical point on ρ defined by a closed set of AIL.[22]

Figure 2 presents the results for the transition states (TS), in the protonation process, found in the complexes Pyr·$n$$H_2O$ with $n = 1-3$. The AIM theory identifies (dashed lines) a ring involving water molecules, the pyridinic nitrogen and the carbon in ortho in the pyridinic ring. In all cases, the transition state shows a protonated nitrogen, with the N−H distance decreasing with n from 1.127 to 1.074 Å; see Figure 2. The values of ρ_b are 0.240, 0.270 and 0.280 au for $n = 1-3$, respectively. The increase of ρ_b and its relationship with the bond order explains the decrease of N−H distances. In the three cases $\nabla^2\rho_b$ is negative, evidencing a shared (covalent) interaction. In addition, we observe a large distance between the carbon in ortho and its hydrogen (C−H), in agreement with the proton transfer observed in the protonated structures.[13] However, this distance decreases with n from 1.362 to 1.295 Å; see Figure 2. Now, the values of ρ_b are 0.148, 0.159 and 0.174 au, for $n = 1-3$, respectively. The increase of ρ_b explains the decrease of the C−H distances. $\nabla^2\rho_b$ is negative, evidencing a covalent interaction.

It is interesting to consider the molecular similarity between the transition states and the solvated and protonated structures. Thus, we have performed molecular similarity calculations using the Carbó-like molecular similarity index defined in the molecular matching protocol of the Hex package.[24] A deep analysis of the Carbó similarity index can be found in ref 28. In Hex, each molecule is represented using 3D parametric functions (based on expansions of real orthogonal spherical polar basis functions) encoding surface shape, electrostatic charge and potential distributions. Hex performs molecular docking and matching by overlapping the parametric functions for the involved molecules.[25] Similarity is determined in the basis of the overlap results, using a normalized overlap volume scaled in the interval [−1000, 0]. The closer to −1000 the result, the higher the similarity. Table 1 shows that for the complexes with one, two, and three water molecules, the transition state is structurally closer to the protonated than to the solvated structure.

TABLE 1: Carbó-like Molecular Similarity Indices As Determined by the Package Hex.[24,a]

n	S-TS	P-TS
1	−803.6	−856.8
2	−815.1	−831.8
3	−804.7	−820.2
4	−798.4	−827.7
5	−754.9	−790.4

[a] The indices are defined in the interval [−1000, 0], with larger negative values meaning higher similarity. The table shows the results of comparing the most stable solvated (S) and protonated (P) structures with the rate determining (highest activation energy) transition state (TS). Pyr·$n$$H_2O$ complexes with $n = 1-5$ are considered.

For the Pyr·$n$$H_2O$ complexes with $n = 4-5$, Figures 3 and 4 show the two transition states (TS_a, TS_b) found, as well as the intermediate solvated minimum. The existence of two transition states is in agreement with the behavior suggested by the vibrational frequencies found for solvated and protonated structures.[13] In these complexes, two rings involving water molecules are found (see Figures 3 and 4), as evidenced by the existence of two RCP's. These rings are similar to the previously found for the solvated and protonated forms.[13] The first ring involves the pyridinic nitrogen, whereas the second is formed by water molecules. As shown in Figures 3 and 4, TS_a involves a proton transfer in the second ring, whereas TS_b corresponds to a proton transfer in the first one. In other words, TS_a represents a concerted proton transfer between the ring of water molecules. On the other hand, TS_b corresponds to the transfer of a proton from a water molecule to the pyridinic nitrogen, and to the abstraction of the proton of the carbon in ortho by another water molecule. These mechanisms of proton transfer fall in the framework of the proton and hydroxyl mobility between hydrogen bonded water molecules, traditionally described by the Grotthuss structural diffusion mechanism.[29] The mobility of the H_3O^+ and the OH^- ions in aqueous solution have been analyzed in the framework of dynamic Carr−Parrinello, ab initio path integral simulations,[30] considering each ion plus 31 water molecules. These studies have shown that the transport mechanisms for H_3O^+ and OH^- are clearly different, but both involve proton transfers between neighbor

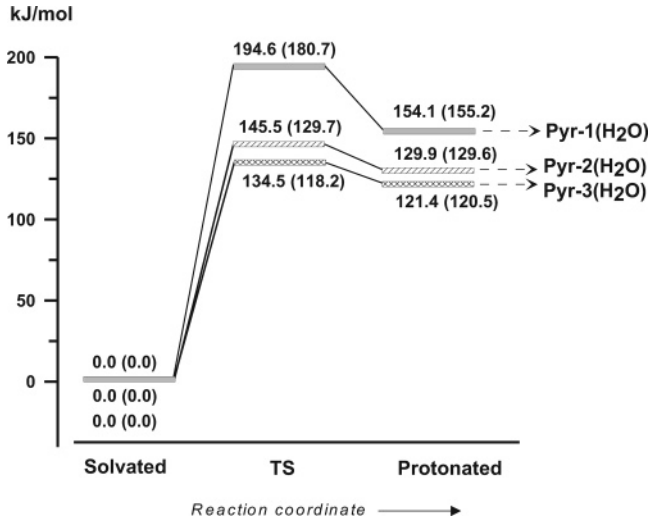

Figure 5. Energetic profile of the reaction path from the solvated to the protonated structure of pyridine in clusters of water molecules, Pyr·nH$_2$O with $n = 1-3$. Total energy differences are shown. In parentheses are total energy differences including the effect of the zero point energy (ZPE). All data are in kJ mol^{-1}.

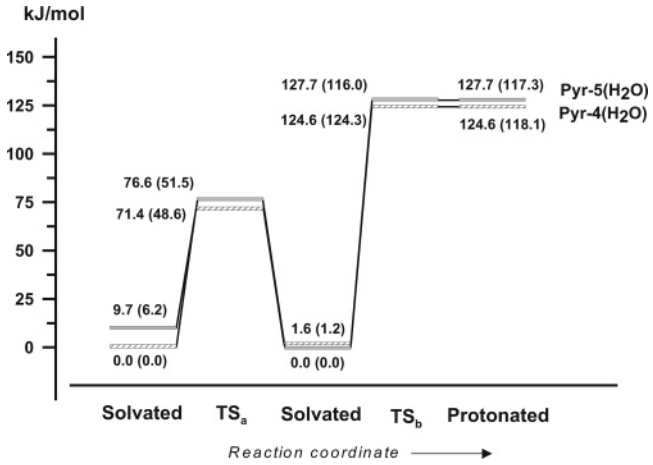

Figure 6. Energetic profile of the reaction path from the solvated to the protonated structure of pyridine in clusters of water molecules, Pyr·nH$_2$O with $n = 4-5$. Total energy differences are shown. In parentheses are total energy differences including the effect of the zero point energy (ZPE). All data are in kJ mol^{-1}.

water molecules. Our present results are obtained with a smaller number of water molecules. However, the present ionization mechanism, leading to protonated pyridine, involves a proton transfer between water molecules, along hydrogen bonds, due to an interconversion between covalent and hydrogen bonds similar to that observed in ref 30.

Respect to the new solvated structure found between TS$_a$ and TS$_b$ (central case in Figures 3 and 4) an interesting difference is found between the complexes with four and five water molecules. For the complex with four water molecules, Figure 3 shows that the AIM theory identifies several bonding interactions (dashed lines) involving pyridine and the water cluster. These are simple interactions, because no atom is involved in more than one bond. In this complex, only two rings are found, as evidenced by its RCP's. However, when five water molecules are available, two atoms are involved in a double bonding interaction; see Figure 4. One of the atoms is the pyridinic nitrogen. This is bonded to protons of two water molecules. The first bond (N···H distance of 1.834 Å) has a value of the Laplacian of the electron density at the BCP, ρ_b, of 0.039 au. The other (N···H distance of 2.494 Å) has a $\rho_b =$ 0.009 au. In both cases $\nabla^2\rho_b$ is positive, evidencing a closed-shell interaction, typical of hydrogen bonds. Also, because the ρ_b is related to the concept of bond order,[22] the higher value for the first bond explains the difference in bonding distances. The AIM analysis also identifies a water molecule where the lone electron pairs of oxygen are used to form two different bonds with another two water molecules; see Figure 4. These bonds exhibit O···H distances of 1.828 Å and 2.013 Å, respectively. The corresponding ρ_b values are 0.023 au and 0.026 au. In both cases, $\nabla^2\rho_b$ is positive, as it should be in a hydrogen bond. The difference of ρ_b explains again the difference in bond lengths. In the present structure, five rings are found, as evidenced by the corresponding RCP's. The higher number of hydrogen bonds suggests that this new solvated structure could be more stable than the original one obtained in ref 13.

The energetic profile for the protonation reaction of pyridine in the water clusters is determined. Thus, we follow forward and backward the reaction coordinate from the obtained transition states, identifying the minima reached. The results are shown in Figures 5 and 6. Figure 5 shows the energetic relationship between the stationary points in the path going from the unprotonated to the protonated Pyr·nH$_2$O complexes, with $n = 1-3$. We observe that the activation energy, E_a (measured from the bottom of the potential well), decreases from 194.6 to 134.5 kJ mol^{-1}, when going from one to three water molecules. In addition, we consider the energy variation measured from the lowest vibrational energy level, i.e., internal energy variations at a temperature of 0 K (ΔU_0). Thus, we evaluate the zero point energy, ZPE, for each stationary point, incorporating it to the total energy. The corresponding ΔU_0 values are shown (in parentheses) in Figure 5. As for E_a, we observe a decrease of the activation ΔU_0 when going from one to three water molecules, in this case from 180.7 to 118.2 kJ mol^{-1}. On the grounds of the transition-state theory, this decrease in energy is correlated with an increase of the rate constant for the protonation process. In short, the protonation rate increases with the number of water molecules.

The energetic profiles for the protonation processes in the Pyr·nH$_2$O complexes, with $n = 4$, 5 are shown in Figure 6. For the complex with four water molecules the new solvated structure, shown as the central case in Figure 3, is slightly less stable than the solvated structure determined in ref 13. The protonated structure is reached from this new solvated structure through TS$_b$, with an activation barrier, $E_a/\Delta U_0$, of 123.6/123.1 kJ mol^{-1}, respectively; see Figure 6. Therefore, for this complex, protonation occurs in two steps through the TS$_a$ and TS$_b$ transition states. The second step, the higher in energy, is the rate determining.

In the case of the Pyr·5H$_2$O complex, the situation differs. Now, the new solvated structure, central case of Figure 4, becomes the total energy minimum (as the structural results suggested), being 9.7 kJ mol^{-1} below the original solvated structure. This result is in agreement with previous findings showing that three-dimensional cage-like structures involving multiple rings are the lowest energy conformers in the water heptamer and octamer.[31] In this case, the activation barrier for protonation, $E_a/\Delta U_0$, reaches 127.1/117.3 kJ mol^{-1}, respectively; see Figure 6. Here, protonation involves a single step. Because the formation of compact structures similar to the solvated structure of Figure 4 is easier as the number of water molecules increases, it seems that protonation of pyridine from a solvated structure in large water clusters should involve a one-step mechanism, as the one found here. The existence of this new structure makes it necessary to revisit the exponential variation of ΔU_0 versus the number of water molecules, n, found in ref

TABLE 2: Fundamental Frequencies of Vibration in the Pyr·nH$_2$O Complexes for the Normal Mode Corresponding to the Reaction Coordinate, in the Transition State Leading to the Protonated Structure, and the Own Protonated Structure (All Data in cm^{-1})

n	TS_b	protonated
1	−1433.6	89.6
2	−974.3	65.2
3	−663.8	34.4
4	−121.2	28.0
5	−67.2	18.9

13. Thus, we have refitted the ΔU_0 data using the new ΔU_0 value for the Pyr·5H$_2$O complex (117.3 kJ mol^{-1}). The result yields an exponential variation (A exp[B/n]) with $A = 108.0$ kJ mol^{-1} and $B = 0.3614$, with correlation coefficient $R = 0.9984$. These results can be compared to the previous $A = 105.6$ kJ mol^{-1} and $B = 0.3888$, with correlation coefficient $R = 0.9931$. The higher value of R indicates a better correlation. However, much more clear is the comparison of the residual sum of squares. The old fit provides a value of 16.1 (kJ mol^{-1})^2, which can be compared to the 3.2 (kJ mol^{-1})^2 obtained now. Clearly, the new ΔU_0 datum fits better in the exponential correlation than the previous value.

Although not directly comparable, it is interesting to remark that this decrease of ΔU_0 with n parallels the decrease of both experimental and theoretical stepwise hydration energies of NaXNa(H$_2$O)$_n^+$ (with X = I, Cl) when going from one to four water molecules.[32] Also, a decrease with n was experimentally found by Hiraoka el al.,[33] for the stepwise hydration values of $\Delta G°$ and $\Delta H°$ in halide ions (F^-, Cl^-, Br^-, I^-), when the number of water molecules goes from one to ten.

For the complexes with four and five water molecules, Figure 6 shows that energetically the protonation transition state, TS_b, is very close to the protonated structure. The molecular structures of the complexes with four and five water molecules are compared using the similarity index implemented in the Hex package.[24,25] Table 1 shows that the rate determining transition state (TS_b) is always closer to the protonated than to the solvated structure. This fact can be explained by considering the vibrational frequency corresponding to the motion along the reaction coordinate. Table 2 collects the vibrational frequencies for the transition states leading to the protonated structures, and the corresponding frequencies for the resulting protonated complexes. It can be observed that the absolute frequency value for the transition states decreases greatly from 1433.6 cm^{-1} (Pyr·H$_2$O complex) to 67.2 cm^{-1} (Pyr·5H$_2$O complex). In addition, the corresponding frequency in the protonated complex, decreases also from 89.6 to 18.9 cm^{-1}. Therefore, the difference of vibration frequencies between the TS and the protonated structure decreases when the number of water molecules in the complex increases. Because the frequency is proportional to the second derivative of the potential energy (the total energy within the Born−Oppenheimer approach) with respect to the vibrational coordinate, it is a measure of the curvature of the potential energy hypersurface. Low values indicate a flat hypersurface in the direction of the considered motion (vibration). Thus, a low-frequency value for TS_b and for the protonated structure means that the motion along the reaction coordinate is associated with a small change of total energy. Therefore, the decrease in the difference of frequencies observed in Table 2 with the number of water molecules (n) must translate as a smaller difference between the total energies of the transition state and the protonated structures with n, as observed in Figures 5 and 6. In particular, for the complex with five water molecules the difference in energy is so small (see Figure 6) that it is totally washed out by the thermal energy ($RT = 2.479$ kJ mol^{-1} at 298.15 K).

TABLE 3: Gibbs Energy Variation between the Most Stable Solvated and Protonated Forms of Pyridine in Water Clusters (Pyr·nH$_2$O), as a Function of the Number of Water Molecules (n)[a]

n	ΔG (kJ mol^{-1})	pK_a
1	3.8	−0.66
2	3.7	−0.65
3	4.6	−0.81
4	−1.6	0.28
5	−13.4	2.35

[a] ΔG is obtained as G(protonated) − G(solvated). Data obtained at the B3LYP/cc-pVDZ level at a temperature of 298.15 K and at a pressure of 1atm. The table includes the pK_a for each protonated complex. Note that with our definition of ΔG, eq 1, the pK_a should be obtained as − log exp[+$\Delta G/RT$].

To gain some insight in the thermodynamics of the protonation process, differences of Gibbs energy between the most stable solvated and protonated complexes have been thermostatistically computed. The results at a temperature of 298.15 K and at a pressure of 1 atm are collected in Table 3. The sign of ΔG indicates that only when the number of water molecules is greater than three is protonation spontaneous. This result is in agreement with those in ref 13, showing a structurally different behavior when the number of water molecules is greater than three. In addition, the pK_a for the protonation reaction has been calculated for the different complexes and included in Table 3. It is seen that the value grows with the number of water molecules, with an increase of an order of magnitude when going from four to five water molecules. The pK_a value for the Pyr·5H$_2$O complex, 2.35, is not far from the value of 5.21[34] for pyridine is aqueous solution at 25 °C. Anyway, description of pyridine in solution will need a more refined model than the supermolecular complexes presented here.

Conclusions

This work presents a theoretical mechanistic study, at the B3LYP/cc-pVDZ level, of the protonation of pyridine in water clusters of increasing size. Supermolecular models of pyridine in water clusters up to five water molecules are considered.

Computation of the protonation reaction paths identifies one transition state for clusters of one to three water molecules. Using a Carbó-like similarity index, we find that the transition states are structurally closer to the protonated forms than to the solvated ones. In addition, the activation energy for protonation decreases, and the reaction rate increases, with the number of water molecules.

In clusters of four and five water molecules two transition states are found, with a new unprotonated (solvated) structure between them. After application of the AIM theory, it is observed that the new solvated structure found for the Pyr·5H$_2$O cluster exhibits several double hydrogen bonds, involving the pyridinic nitrogen and one of the water molecules. The result is a more compact solvated structure than the starting one, bearing a total of five rings involving pyridine and the water cluster. Energetically, for the Pyr·4H$_2$O complex the new solvated structure is less stable than the original one. However, in the Pyr·5H$_2$O case, the new structure becomes the most stable. Therefore, protonation of pyridine exhibits a two-step mechanism in the Pyr·4H$_2$O case, and a one-step mechanism in the Pyr·5H$_2$O complex. In both cases, the rate determining transition

state and the protonated form are very close in energy. Molecular similarity calculations show that the rate determining transition states are closer to the protonated forms than to the solvated ones. Analyzing the variation of vibration frequencies on the reaction coordinate, we find that this effect is due to a very flat potential energy hypersurface on that direction.

In all cases considered, complexes of pyridine with water clusters up to five water molecules, protonation is achieved by a concerted proton transfer between the water molecules. The mechanism involves an interconversion between covalent and hydrogen bonds.

Considering the Gibbs energy variation between the most stable solvated and protonated forms, we find that protonation needs at least four water molecules to become a spontaneous process. In particular, and despite the difference with an aqueous solution, five water molecules are needed to obtain a pK_a value of the same order of magnitude that the one determined for pyridine in water.

Acknowledgment. This work has been supported by the *Junta de Comunidades de Castilla-La Mancha* (grant # PAI-02-001), and the *Universidad de Castilla-La Mancha*.

References and Notes

(1) Niño, A.; Muñoz-Caro, C.; Carbó-Dorca, R.; Gironés, X. *Biophys. Chem.* **2003**, *104*, 417−427.

(2) (a) Cramer, C. J.; Truhlar, D. G. In *Reviews in Computational Chemistry*; Lopkowitz, K. B., Boyd, D. B., Eds.; VCH Publishers: New York, 1995; Vol. 1, Chapter 1. (b) Orozco, M.; Luque, F. J. *Chem. Rev.* **2000**, *100*, 4187−4225. (c) Bandyopadhyay, P.; Gordon M. S. *J. Chem. Phys.* **2000**, *113*, 1104−1109.

(3) Zhan, C.-G.; Landry, D. W.; Ornstein, R. L. *J. Am. Chem. Soc*. **2000**, *122*, 2621−2627.

(4) Lee, C.; Sosa, C.; Novoa, J. J. *Chem. Phys.* **1995**, *103*, 4360−4362.

(5) Lee, C.; Sosa, C.; Planas, M.; Novoa, J. J. *J. Chem. Phys*. **1996**, *104*, 7081−7085.

(6) Milet, A.; Struniewicz, C.; Moszynski, R.; Wormer, P. E. S. *J. Chem. Phys.* **2001**, *115*, 349−356.

(7) White, J. A.; Schwegler, E.; Galli, G.; Gygi, F. *J. Chem. Phys*. **2000**, *113*, 4668−4673.

(8) Conley, C.; Tao, F.-M. *Chem. Phys. Lett.* **1999**, *301*, 29−36.

(9) Tachikawa, M. *Mol. Phys*. **2002**, *100*, 881−901.

(10) Amirand, A.; Maillard, D. *J. Mol. Struct*. **1988**, *176*, 181−201.

(11) Hurley, S. M.; Dermota, T. E.; Hydutsky, D. P.; Castleman, A. W., Jr. *Science* **2002**, *298*, 202−204.

(12) Wang, X. B.; Yang, X.; Nicholas, J. B.; Wang, L. S. *Science* **2001**, *294*, 1322−1325.

(13) Sicilia, M. C.; Muñoz-Caro, C.; Niño, A. *ChemPhysChem.* **2005**, *6*, 139−147.

(14) (a) Niño, A.; Muñoz-Caro, C. *Biophys. Chem*. **2001**, *91*, 49−60; (b) Muñoz-Caro, C.; Niño, A. *Biophys. Chem*. **2002**, *96*, 1−14.

(15) (a) Davidson, W. R.; Sunner, J.; Kebarle, P. J. *J. Am. Chem. Soc*. **1979**, *101*, 1675−1680. (b) Meot-Ner (Mautner), M.; Sieck, L. W. *J. Am. Chem. Soc.* **1983**, *105*, 2956−2961.

(16) (a) Aue, D. H.; Webb, H. M.; Bowers, M. T.; Liotta, C. L.; Alexander, C. J.; Hopkins, H. P. *J. Am. Chem. Soc*. **1976**, *98*, 854−856; (b) Arnett, E. M.; Chawla, B.; Bell, L.; Taagepera, M.; Hehre, W. J.; Taft, R. W. *J. Am. Chem. Soc*. **1977**, *99*, 5729−5738.

(17) Liotard, D. A. *Int J. Quantum Chem*. **1992**, 44, 723−741.

(18) (a) Dewar, M. J. S. *Org. Mass Spectrom*. **1993**, *28*, 305−310. (b) Dewar, M. J. S. *Tetrahedron* **1993**, *23*, 5003−5038.

(19) Holder, A. J.; Evleth, E. M. In *SAM1: General Description and Performance Evaluation for Hydrogen Bonds* in *Modeling the Hydrogen Bond*; Smith, D. A., Ed.; ACS Symposium Series: American Chemical Society: Washington, DC, 1993; pp 113−124.

(20) Ampac 7.0. Semichem, 2000.

(21) Frisch, M. J.; Trucks, G. W.; Schlegel, H. B.; Scuseria, G. E.; Robb, M. A.; Cheeseman, J. R.; Montgomery, J. A., Jr.; Vreven, T.; Kudin, K. N.; Burant, J. C.; Millam, J. M.; Iyengar, S. S.; Tomasi, J.; Barone, V.; Mennucci, B.; Cossi, M.; Scalmani, G.; Rega, N.; Petersson, G. A.; Nakatsuji, H.; Hada, M.; Ehara, M.; Toyota, K.; Fukuda, R.; Hasegawa, J.; Ishida, M.; Nakajima, T.; Honda, Y.; Kitao, O.; Nakai, H.; Klene, M.; Li, X.; Knox, J. E.; Hratchian, H. P.; Cross, J. B.; Adamo, C.; Jaramillo, J.; Gomperts, R.; Stratmann, R. E.; Yazyev, O.; Austin, A. J.; Cammi, R.; Pomelli, C.; Ochterski, J. W.; Ayala, P. Y.; Morokuma, K.; Voth, G. A.; Salvador, P.; J. J. Dannenberg, Zakrzewski, V. G.; Dapprich, S.; Daniels, A. D.; Strain, M. C.; Farkas, O.; Malick, D. K.; Rabuck, A. D.; Raghavachari, K.; Foresman, J. B.; Ortiz, J. V.; Cui, Q.; Baboul, A. G.; Clifford, S.; Cioslowski, J.; Stefanov, B. B.; Liu, G.; Liashenko, A.; Piskorz, P.; Komaromi, I.; Martin, R. L.; Fox, D. J.; Keith, T.; Al-Laham, M. A.; Peng, C. Y.; Nanayakkara, A.; Challacombe, M.; Gill, P. M. W.; Johnson, B.; Chen, W.; Wong, M. W.; Gonzalez, C.; Pople, J. A. *Gaussian 03*, revision B.04; Gaussian, Inc.: Pittsburgh, PA, 2003.

(22) (a) Bader, R. F. W. *Atoms In Molecules. A Quantum Theory*; Oxford University Press: Oxford, England, 1995. (b) Popelier, P. *Atoms In Molecules. An Introduction*; Prentice Hall: Essex, England, 2000.

(23) MORPHY98, a topological analysis program written by P. L. A. Popelier with a contribution from R. G. A. Bone; UMIST, Manchester, England, EU, 1998.

(24) Hex. Version 4.2 by D. Ritchie. University of Aberdeen, Aberdeen Scotland, UK, 2003.

(25) (a) Ritchie, D. W.; Kemp, G. J. L. *J. Comput. Chem.* **1999**, *20*, 383−395. (b) Ritchie, D. W. *Proteins* **2003**, *52*, 98−106.

(26) NPACI Rocks Cluster Distribution. Version 3.0.0. Available from: http://rocks.npaci.edu/Rocks/.

(27) Fernandez-Berridi, M. J.; Iruin, J. J.; Irusta, L.; Mercero, J. M.; Ugalde, J. M. J. *Phys. Chem. A* **2002**, *106*, 4187−4191.

(28) Carbó-Dorca, R.; Robert, D.; Ll. Amat, Girones, X.; Besalú, E. *Molecular Quantum Similarity in QSAR and Drug Design*, Lecture Notes in Chemistry 73, Springer-Verlag: Berlin Heildelberg, 2000.

(29) (a) de Grotthuss, C. J. T. *Ann. Chim*. **1806**, LVIII 54−74. (b) Laidler, K. J.; *Chemical Kinetics*, 3rd ed.; HarperCollinsPublishers: New York, 1987. (c) Pilling, M. J.; Seakins, P. W. *Reaction Kinetics*; Oxford University Press: Oxford, England, 1997.

(30) (a) Marx, D.; Tuckerman, M. E.; Hutter, J.; Parrinello, M. *Nature* **1999**, *397*, 601−604. (b) Tuckerman, M. E.; Marx, D.; Parrinello, M. *Nature* **2002**, *417*, 925−929.

(31) (a) Gruenloh, C. J.; Carney, J. R.; Hagemeister, F. C.; Arrington, C. A.; Zwier, T. S.; Fredericks, S. Y.; Wood, J. T., III; Jordan, K. D. *J. Chem. Phys.* **1998,** *109*, 6601−6614. (b) Ludwig, R. *Angew. Chem., Int. Ed.* **2001**, *40*, 1808−1827.

(32) Blades, A. T.; Peschke, M.; Verkerk, U. H.; Kebarle, P. *J. Am. Chem. Soc.* **2004**, *126*, 11995−12003.

(33) Hiraoka, K.; Mizuse, S.; Yamabe, S. *J. Phys. Chem.* **1998**, *92*, 3943−3952..

(34) Fischer, A.; Galloway, W. J.; Vaughan, J. *J. Chem. Soc. B* **1964**, 3591.